Panchromatic Type II Photoinitiator for Free Radical Polymerization Based on Thioxanthone Derivative

ARTICLE *in* MACROMOLECULES · MAY 2013

Impact Factor: 5.8 · DOI: 10.1021/ma302641d

6 AUTHORS, INCLUDING:

Haja Tar
Université de Haute-Alsace
4 PUBLICATIONS **47** CITATIONS
SEE PROFILE

Christian Ley
Université de Haute-Alsace
55 PUBLICATIONS **499** CITATIONS
SEE PROFILE

Nergis Arsu
Yildiz Technical University
84 PUBLICATIONS **1,376** CITATIONS
SEE PROFILE

Xavier Allonas
Université de Haute-Alsace
206 PUBLICATIONS **2,921** CITATIONS
SEE PROFILE

Macromolecules

Article

pubs.acs.org/Macromolecules

Panchromatic Type II Photoinitiator for Free Radical Polymerization Based on Thioxanthone Derivative

Haja Tar,[†] Duygu Sevinc Esen,[‡] Meral Aydin,[‡] Christian Ley,[†] Nergis Arsu,*[,‡] and Xavier Allonas*[,†]

[†]Laboratory of Macromolecular Photochemistry and Engineering, Université de Haute Alsace, 3 rue Alfred Werner, 68093 Mulhouse, France

[‡]Department of Chemistry, Yildiz Technical University, 34220 Davutpasa, Istanbul, Turkey

Supporting Information

ABSTRACT: A new photoinitiator for free radical photopolymerization, belonging to the thioxanthone derivatives, was synthesized and characterized. It was found that the compound absorbs over the whole UV−vis spectrum with relatively high absorption coefficients. Fluorescence studies reveal that three different singlet excited states are responsible for this absorption. Phosphorescence and laser flash photolysis evidence the formation of a triplet state from which a photoreduction can occur. Consequently, initiating radicals were formed which are able to initiate the photopolymerization of methyl methacrylate in DMF. Finally, the photopolymerization of acrylates was performed in film at different wavelengths such as 392, 476, 532, and 632 nm, emphasizing the possibility to use this novel photoinitiator when panchromatic irradiation is required.

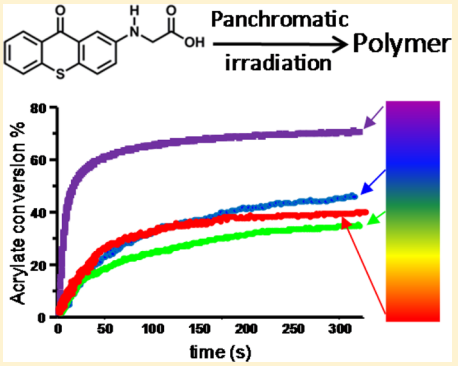

INTRODUCTION

Photoinitiated polymerization is commonly used to cure various monomers including acrylates, methacrylates, epoxides, and vinyl ethers. Many industrial applications were developed using this technology, and photopolymers find developments in coatings on various materials, adhesives, printing inks, restorative dental materials, electronics, and optics.[1−4] Most of these applications are based on photoinitiated free radical vinyl polymerization. This process is based on the absorption of actinic light by a photoinitiator, which can produce primary radical species capable of converting a multifunctional monomer into a cross-linked network. Therefore, in the development of this technology, the photoinitiator plays a very important role. Over the years, several types of photoinitiators have been developed to induce the photopolymerization or photo-cross-linking of acrylated systems.[5,6]

Type II photoinitiators are one of the mostly used class of photoinitiators. They have been deeply studied, and their reactivity involves a triplet excited state which reacts with hydrogen donors to produce initiating radicals (Scheme 1).[7,8] As co-initiators, amines,[9,10] ethers,[11] and thiols[12,13] are the most widely used hydrogen donors. In general, the bimolecular photoreaction leads to the formation of one initiating radical and a second radical which is not an efficient initiating radical.[8,14]

Typical type II photoinitiators include benzophenone,[15] camphorquinone,[10] and thioxanthone derivatives which mainly absorb in the UV part of the electromagnetic spectrum.[16,17] For irradiation in the visible region, one has to use some dyes such as rose bengal, eosin, safranine, and methylene blue.[18,19] This allows to extend the actinic region from the blue to the red depending on the absorption spectrum of the dye. However, there is still only rare examples of photoinitiating systems which exhibit a panchromatic absorption spectrum, rendering possible the use of the same photoinitiator for RGB (red, green, and blue) applications.[20,21]

The compounds based on the thioxanthone (TX) chromophore are among the most used photoinitiators for free radical polymerization. Many efforts were devoted to the development of new structures of thioxanthones in order to obtain high photoinitiating efficiencies. By example, thiol[22,23] and carboxylic acid[24,25] derivatives of thioxanthone have been reported to initiate photopolymerization without use of additional co-initiator. However, thioxanthone derivatives exhibit UV−vis absorption spectra that are mainly located in the short wavelength region of the electromagnetic spectrum (250−410 nm). Recently, a thioxanthone derivative which

Scheme 1. Reaction Mechanism for Type II Photoinitiators for Free Radical Photopolymerization

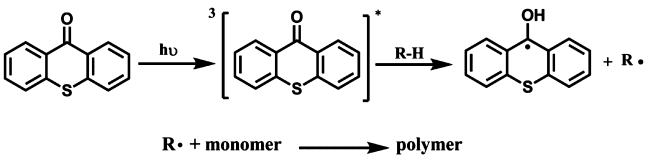

Received: December 26, 2012
Revised: April 9, 2013

   dx.doi.org/10.1021/ma302641d | *Macromolecules* XXXX, XXX, XXX−XXX

absorbs over the whole UV−vis spectrum was proposed,[26] opening the way to produce panchromatic photoinitiator.

As part of our continuous interest in developing new photoinitiating systems, we report the synthesis of novel carboxylic acid group substituted thioxanthone (TX-NPG). The major feature of this compound is a broad, intense absorption spectrum which extends from the UV to the red region. It will be shown that TX-NPG is an efficient photoinitiator for free radical polymerization, and it initiates the polymerization in the absence and presence of hydrogen donor. This efficiency is drastically enhanced in the presence of hydrogen donors. These results pointed out the role that TX-NPG may find in a variety of practical applications.

EXPERIMENTAL SECTION

Materials. Thiosalicylic acid (98%, Aldrich), sulfuric acid (H_2SO_4), *N*-phenylglycine (NPG, 95%, Aldrich), thioxanthone (Aldrich), *N,N*-dimethylformamide (DMF, 99.5%, Meck), ethanol (Merck), tetrahydrofuran (THF, Merck), *N*-methyl-diethanolamine (MDEA, 99%. Aldrich), ethanol (96%, Merck), diethyl ether (Merck), and Na_2CO_3 (Merck, anhydrous 99.99%) were used as received. Methyl methacrylate (99+%, Aldrich) was washed with 5% aqueous NaOH solution and dried over Na_2SO_4 just before use. Bisphenol A ethoxylate diacrylate (EBPOA, SR 349) was used as a viscous monomer (viscosity of η = 1600 mPa s at 25 °C) and was obtained from Sartomer. All other reagents were purchased from Merck and used as received.

Synthesis of TX-NPG. Thiosalicylic acid (1.6 g, 10.3 mmol) was slowly added to concentrated sulfuric acid (15 mL), and the mixture was stirred for 5 min to ensure thorough mixing. *N*-Phenylglycine (6.64g, 44 mmol) was added slowly to the stirred mixture over a period of 30 min. After the addition, the reaction mixture was stirred at room temperature for 1 h and then at 80 °C for 15 h, after which it was left to stand at room temperature overnight. The resulting mixture was poured carefully with stirring into a 10-fold excess of boiling water, and it was then boiled further for 5 min. The solution was cooled and filtered. The residue was washed with diethyl ether to remove impurities. Yield 80%. $C_{15}H_{11}O_3SN$: 285 g/mol. ^{1}H NMR (MeOD, 500 MHz) δ ppm: 2.09 (s, 2H, CH_2), 2.14 (s, 1H, NH), 6.6−6.8 (m, 2H, aromatic), 7.2−7.3 (m, 2H, aromatic), 7.4−7.6 (m, 1H, aromatic), 7.7−7.9 (m, 1H, aromatic), 8.1−8.2 (m, 1H, aromatic). FT-IR (ATR): 3355 (N−H stretching), 2919 (aliphatic C−H stretching), 1695 (C═O, acid), 1621(C═O, ketone), 1589 (aromatic C═C stretching) cm^{-1}. Elemental analysis: C: 63.16%, H: 3.86%, S: 11.23% (calculated); C: 6.94%, H: 4.02%, S: 11.68% (found).

Photopolymerization. Appropriate solutions of the photoinitiator which have different optic densities were prepared in the presence of methyl methacrylate with and without *N*-methyldiethanolamine. They were irradiated in a photoreactor consisting of a 400 W medium-pressure mercury lamp and a water cooling system for 15 min in either air or nitrogen atmosphere. The poly(methyl methacrylate) which formed at the end of the irradiation was precipitated in a 10-fold excess of methanol and dried *in vacuo*. All other polymerizations using different concentrations were performed under identical experimental conditions unless otherwise stated. For the experiments under nitrogen, the same solutions which were put into a Pyrex tube were flushed with dry nitrogen. Polymerization yields were calculated for all samples gravimetrically.

Instrumentation. The curing kinetics were determined by the real-time FTIR technique using a Vertex 70 (Bruker) equipped with a MCT detector working in the rapid scan mode, allowing around 8 scans/s collection rate (time resolution of 0.116 s) with 4 cm^{-1} spectral resolution. The spectra were recorded between 600 and 3900 cm^{-1}. The samples were irradiated either by LED emitting at 392 nm (Prizmatix) or with laser emitting diodes emitting at 473, 532, or 635 nm (Roithner Lasertechnik GmbH). These sources of light were adapted to the FT-IR spectrometer by means of a light guide. Intensity effects were performed by attenuation of the light with neutral UV density filters in the range 0.6−40 mW/cm^2. Before each experiment, the actual incident irradiation intensity on the sample was measured with a calibrated UV−vis spectrophotometer (Ocean Optics USB4000). The monomer used was a diacrylate SR 349 (Sartomer), containing TX-NPG at a concentration of 10^{-3} M, 4 wt % DMF. NPG was used as co-initiator at a concentration of 5×10^{-3} M.

The conversion of the monomer was followed at 1640 cm^{-1}:

$$\text{conv} = 100 \times (A_0 - A_t)/A_0 \quad (1)$$

where A_0 and A_t are the absorbance of double bonds at 1637 cm^{-1} before irradiation and after time t, respectively.

To prevent the diffusion of oxygen into the sample under exposure, laminate experiments were done by placing the resin between two polypropylene films and two BaF_2 crystal windows. The thickness of the sample was adjusted using a 50 μm Teflon spacer.

Gel permeation chromatography (GPC) (Agilent 1100) analyses of the polymers were performed with a setup consisting of a pump (Waters) and four Ultrastyragel columns of different porosities. Tetrahydrofuran (THF) was used as the eluent (flow rate 0.3 mL min^{-1}), and the detection was carried out with the aid of a differential refractometer. The number-average molecular weights were determined using polystyrene standards.

UV−vis spectra (Cary 4000, Varian) were measured at room temperature in a 1 cm quartz cuvette, using dimethylformamide as solvent. The ^{1}H NMR spectrum was taken on Bruker 500 MHz instrument using MeOD as solvent. The IR spectrum was taken on Nicolet 6700 FT-IR spectrophotometer. Fluorescence experiments were performed using a FluoroMax-4 spectrofluorometer (HORIBA Jobin Yvon) coupled with a time-correlated single photon counting (TCSPC) for lifetime determination. 374 and 456 nm NanoLEDs (duration 0.2 and 1.7 ns, respectively) were used as pulsed excitation source leading to a time resolution of around 200 ps. The measurements were performed in methanol solution under argon. Femtosecond time-resolved transient absorption experiments were performed with a CDP Corp. Excipro pump−probe apparatus. Femtosecond laser excitation wavelength was adjusted to 355 nm by fourth-harmonic generation of a collinear 800 nm/100 fs pumped optical parametric amplifier (CDP2017, CDP Corp). The 100 fs laser pulses at 800 nm were provided by a Spectra-Physics Tsunami Ti:Sa oscillator coupled to a Spitfire pro Spectra-Physics regenerative amplifier. The resulting pump−probe cross-correlation of the setup was found to be about 250 fs. The phosphorescence spectrum was recorded on a Fluoromax-P spectrofluorometer (HORIBA Jobin Yvon) at 77 K using 3 mm (inner diameter) quartz tubes inside a quartz liquid nitrogen dewar.

Laser flash photolysis setup was based on a Nd:YAG laser (Powerlite 9010, Continuum), operating at 10 Hz. The transient absorption analysis system (LP900, Edinburgh Instruments) uses a 450 W pulsed Xe arc lamp, a Czerny−Turner monochromator, a fast photomultiplier, and a transient digitizer (TDS 340, Tektronix). The photoinitiator was dissolved in methanol at a concentration such that the absorbance was about 0.5 at the excitation wavelength (355 nm).

RESULTS AND DISCUSSION

TX-NPG (2-(9-oxo-9*H*-thioxanthen-2-ylamino)acetic acid) was synthesized by the reaction thiosalicylic acid with *N*-phenylglycine (NPG) according to a modified literature procedure (Scheme 2).[24,27] The structure of TX-NPG was confirmed by spectroscopic analysis (see Experimental Section).

Scheme 2. Synthesis of TX-NPG

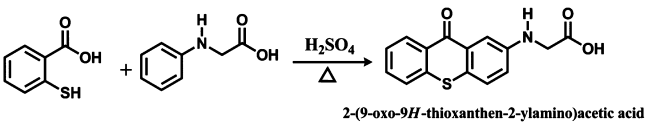

dx.doi.org/10.1021/ma302641d | Macromolecules XXXX, XXX, XXX−XXX

Absorption characteristics of the photoinitiator were examined by UV spectroscopy. Figure 1 demonstrates the

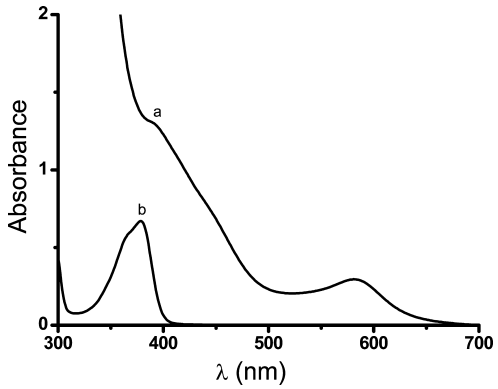

Figure 1. Absorption spectra of (a) TX-NPG (8×10^{-4} M) and (b) TX (5×10^{-5} M) in DMF.

comparison of UV spectra of TX-NPG with the parent compounds thioxanthone (TX) in DMF. Interestingly, TX-NPG exhibits strong absorption in the visible range which extends from the UV to the red (λ > 600 nm), while TX chromophore is transparent above 410 nm.

TX-NPG possesses absorption across the whole visible region and high molar absorptivities with two peaks at 392 nm (ε = 1664 L mol^{-1} cm^{-1}) and 583 nm (ε = 443 L mol^{-1} cm^{-1}). This very peculiar behavior has been already detected in other TX derivatives. Indeed, such absorption spectra have been published for thioxanthone carboxylic acid[28] and sodium fluorenecarboxylate−thioxanthone.[26] The involvement of a hydrogen bonding has been proposed to explain such unusual behavior. In the case of TX-NPG, an intramolecular or intermolecular hydrogen bond is expected as well, as confirmed by the disappearance of the red-shifted absorption band when triethylamine is added to a solution of TX-NPG (see Supporting Information). Computational prediction of the absorption properties of thioxanthone derivative is known to be quite tricky. High level of theory has been recently used to investigate the photophysics of thioxanthone.[29,30] However, such highly demanding computation cannot be performed for TX-NPG.

The high molar absorptivity makes the thioxanthone derivative very attractive as a photoinitiator. Figure 2 shows the fluorescence spectra of TX-NPG in methanol at room temperature. Different emission bands can be detected as resulting from three different singlet excited states. A nearly mirror-image-like relation exists between the excitation and emission spectra whatever the absorption band, evidencing that the absorption spectrum could not be attributed to an artifact. A clear proof of the existence of three emissive states is given by the fluorescence excitation spectra that match quite well the three absorption band. These three emissive singlet states have energies that can be calculated from the intercept between normalized absorption and emission bands, and the lifetimes can be measured by single photon counting: a first excited state S_1 of 2.0 eV and a lifetime of 12 ns covers the green and red region. A second absorption in the blue region corresponds to an excitation to a S_2 singlet state of 2.6 eV, with a lifetime of 3−5 ns. The UV part of the absorption spectrum corresponds to a S_3 excited state which has an energy of 3.1 eV and a lifetime of 0.16 ns. The singlet excited states S_2 and S_1 are much longer

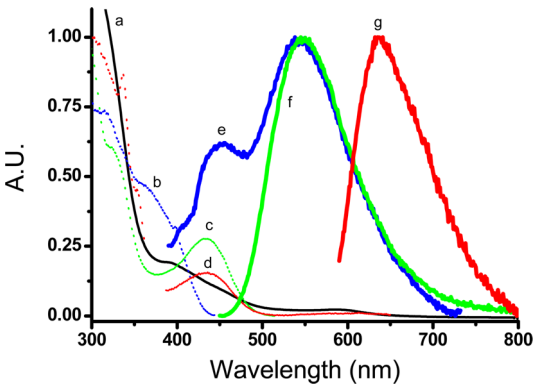

Figure 2. (a) Absorption spectrum of TX-NPG in DMF compared to excitation spectra recorded at emission wavelengths of (b) 452, (c) 526, and (d) 740 nm. Emission spectra obtained by excitation at (e) 374, (f) 445, and (g) 580 nm.

than expected for TX.[31] This is probably due to the fact that intersystem crossing to the triplet state is not favorable from S_2 and S_1.

Femtosecond time-resolved pump−probe experiments performed in DMF solutions confirm the existence of ultrafast kinetics in the photophysics of TX-NPG. Broad and spectrocopically unresolved transient absorption was detected. However, singular value decomposition allowed a good analysis of these spectrotemporal data.[32−34] The best fit of the three first weighted orthogonal kinetics leads to three time constants of 9.3 ps, 75 ps, and 6.2 ns and to a step function (see Figures S2 and S3 in Supporting Information). The two last components correspond to the 3−5 and 12 ns TCSPC values (the last one is too long to be resolved by the femtosecond setup and leads to the step function). Moreover, the obtained two short components (9.3 and 75 ps) confirm the ultrafast kinetics of 150 ps not fully resolved in TCSPC fluorescence measurement, which could be ascribed to ultrafast internal relaxation from S_3 to lower excited states of TX-NPG.

Interesting information about triplet state can be obtained from phosphorescence spectrum of the initiator measured in ethanol at 77 K upon excitation with 390 nm light (see Figure 3). The (0,0) emission bands for TX-NPG is located at 488 nm, corresponding to an approximate triplet energy of 245 kJ/mol. Interestingly, the energy of the triplet state is lower than that of S_1. Moreover, phosphorescence measurements are

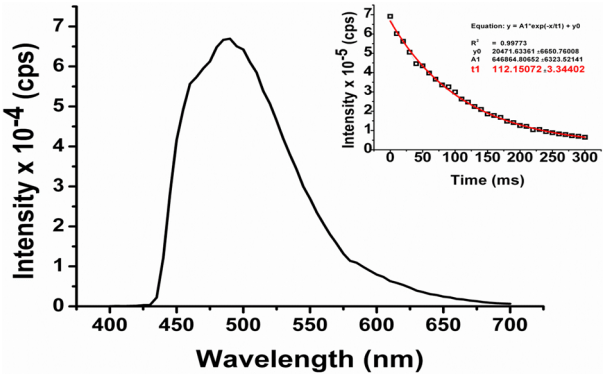

Figure 3. Phosphorescence emission spectrum of TX-NPG in ethanol at 77 K upon excitation at 390 nm. Inset: corresponding decay curve.

dx.doi.org/10.1021/ma302641d | Macromolecules XXXX, XXX, XXX−XXX

useful to gain information on the triplet configurations of TX-NPG.

The phosphorescence emission possesses a long lifetime of 112 ms. It is known that the phosphorescence lifetime for $n\pi^*$ triplets is significantly shorter (in the order of several milliseconds) compared with $\pi\pi^*$ triplets (more than 100 ms).[25] Consequently, the results obtained from the phosphorescence measurements indicate a $\pi\pi^*$ like nature of the lowest triplet state.

Assessment of triplet formation can be obtained by laser flash photolysis in DMF, at room temperature and under argon. After laser flash, a transient appears with similar features than TX[8,35,36] and mercaptothioxanthone[22] (Figure 4). This

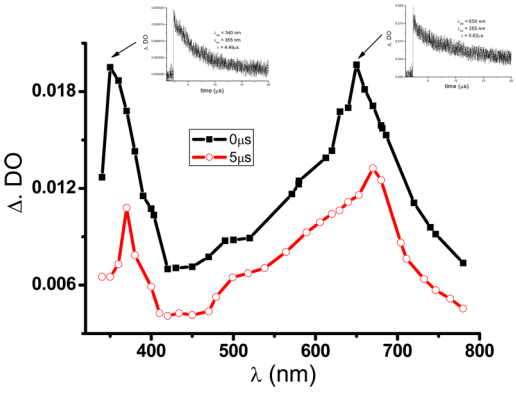

Figure 4. Transient absorption spectra of nitrogen-saturated DMF solution of TX-NPG (2.24×10^{-4} M) recorded at 0 and 5 μs after laser flash. Inset: corresponding decay curves recorded at 340 and 650 nm.

spectrum shows two maxima at 650 and 340 nm. The peak at 650 nm was safely attributed to the triplet−triplet absorption of TX-NPG because of the similarities with the triplet−triplet spectra of TX and TX-SH. This transient is quenched by oxygen with a rate constant of about 10^9 M^{-1} s^{-1}. The peak at 340 nm was attributed in the literature to an overlap between triplet−triplet absorption of thioxanthone and the ketyl radical.[37]

In the absence of quencher, the corresponding band of TX-NPG is predominantly attributed to the triplet state. The corresponding lifetime was found to be about 4.3 μs.

The whole energy diagram was proposed in Figure 5, showing three different singlet excited states that could lead to fluorescence or that can populate the triplet state though

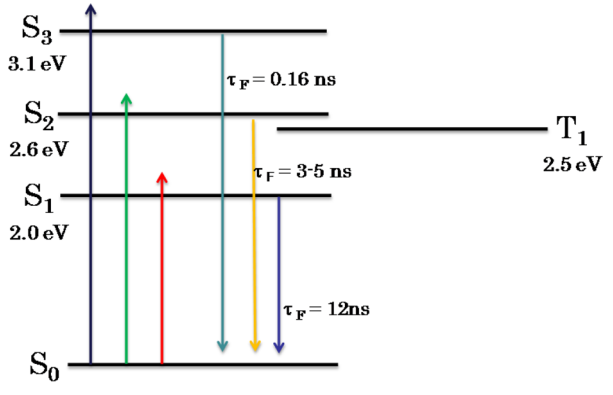

Figure 5. Proposed energy level diagram for TX-NPG.

intersystem crossing. A photoreaction is expected to be favorable from this relatively long-lived triplet state. Indeed, the triplet state of TX-NPG was found to be quenched by *N*-phenylglycine NPG as hydrogen donor. Stern−Volmer analysis leads to a bimolecular quenching rate constant of 2.4×10^7 M^{-1} s^{-1}.

The involvement of a decarboxylation process during the photolysis of TX-NPG was addressed by detection of CO_2 using a procedure described in the literature.[25] 1 mL of a DMF solution of TX-NPG (5 mM) was placed in Pyrex tube which was connected to another tube containing an aqueous solution of Na_2CO_3 (0.67 mM) and one drop of phenolphthalein solution (0.025 mM). After 55 min of irradiation with a xenon lamp (175 W/m^2 UVB and 487 W/m^2 UVA) the pink color of the phenolphthalein solution disappeared, evidencing the formation of CO_2. It has been already shown for this kind of thioxanthone derivative that self-quenching from the triplet state could lead to the formation of initiating radical during the decarboxylation process (Scheme 3). Unfortunately, the important signal/noise ratio of the transient does not permit to determine accurately the kinetics of the triplet state decay.

Scheme 3. Reaction Mechanism of TX-NPG

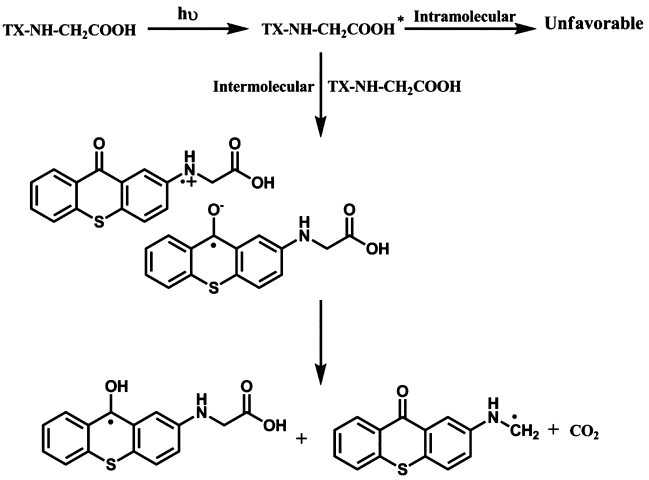

The production of radical under excitation of TX-NPG was demonstrated by photopolymerization experiments. TX-NPG and methyl methacrylate (MMA) were dissolved in DMF and irradiated for 15 min, either in a nitrogen or air atmosphere, with or without *N*-methyldiethanolamine (MDEA) as co-initiator. Resulting monomer conversions and molecular weights are compiled in Table 1.

As can be seen, in the presence of dissolved oxygen and with no additional co-initiator, TX-NPG appears to be an efficient photoinitiator. The efficiency decreases with increasing the absorbance of TX-NPG. This is attributed to a competition between intermolecular processes arising for the photoreaction of the triplet state of TX-NPG with a TX-NPG ground state or a molecule of oxygen.

As can be seen from Table 1, the conversion percentage value (OD = 0.25) was 6.9 in air whereas it was 4.7 in a nitrogen atmosphere, and when the initiator concentration increased (OD = 0.50), the conversion percentage values increased to 10.6 in air and to 6.6 in a nitrogen atmosphere. With a further increase in the initiator concentration to OD = 1.41, the conversion percentage values dropped down to 6.5 in air but still increased in nitrogen atmosphere (conv = 9.3%).

dx.doi.org/10.1021/ma302641d | *Macromolecules* XXXX, XXX, XXX−XXX

Table 1. Photoinitiated Polymerization of Methyl Methacrylate (MMA) by TX-NPG and TX in DMF[a]

run	photoinitiator OD	[MDEA] (mol L−)	N_2	conv (%)	$R_p \times 10^5$ (mol L^{-1} s^{-1})	$M_n \times 10^{-4}$ (g mol^{-1})
1	0.25	−	−	6.9	35.7	5.54
		−	+	4.7	24.6	9.97
		+	−	9.2	48.0	5.10
2	0.50	−	−	10.6	55.1	5.62
		−	+	6.6	34.2	7.07
		+	−	10.5	54.6	3.76
3	0.75	−	−	8.4	43.7	5.24
		−	+	7.5	39.2	9.63
		+	−	12.6	65.4	4.02
4	1.00	−	−	8.0	41.4	5.94
		−	+	9.0	46.7	9.12
		+	−	15.6	81.2	3.42
5	1.41	−	−	6.5	33.6	4.82
		−	+	9.3	48.6	7.34
		+	−	16.9	88.0	3.18
6[b]	0.75	−	−	0		
		+	−	3.5	18.1	

[a]λ = 350 nm; irradiation time = 15 min; photoinitiator = TX-NPG and MDEA = *N*-methyldiethanolamine; determined by GPC according to linear polystyrene standards [MMA] = 4.68 mol L^{-1}, [DMF] = 6.63 mol L^{-1}, and [MDEA] = 10^{-2} mol L^{-1}. [b]TX was used as initiator.

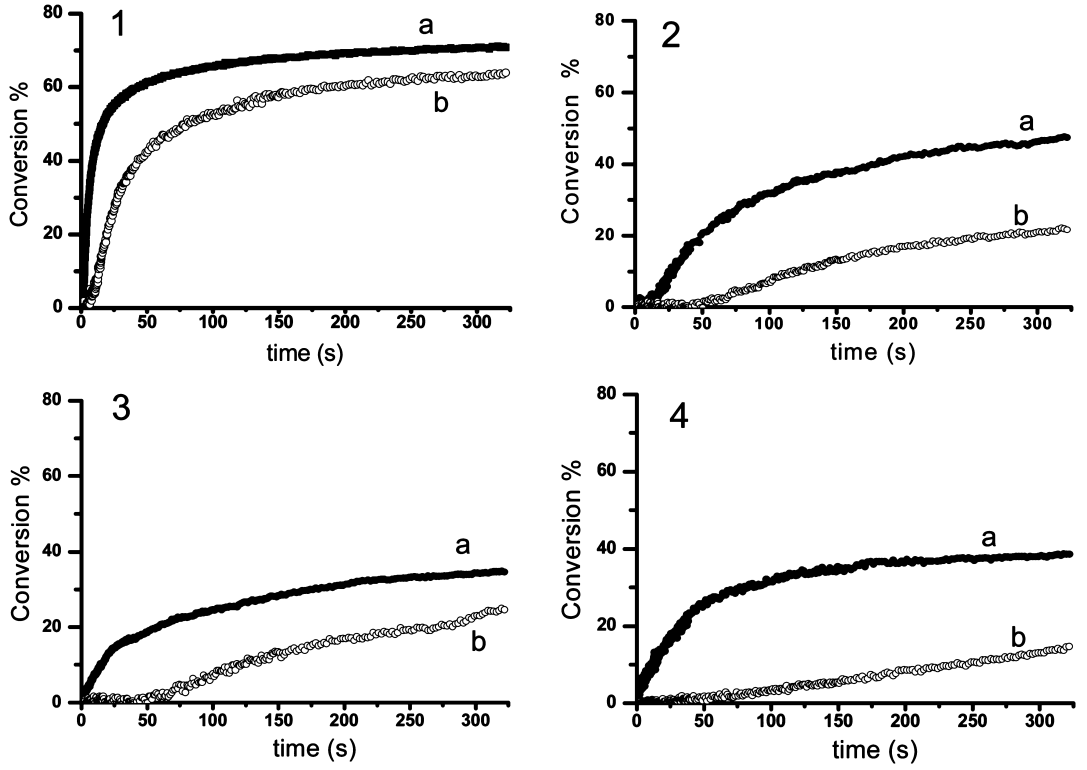

Figure 6. Conversion curves using TX-NPG as radical photoinitiator (a) with and (b) without co-initiator, at (1) 392 nm, (2) 473 nm, (3) 532 nm, and (4) 632 nm. Monomer SR 349, [TX-NPG] = 10^{-3} M, [NPG] = 5×10^{-3} M as co-initiator, 4 wt % DMF.

During the photopolymerization reaction, due to decarboxylation, CO_2 elimination occurs, and this helps to reduce the inhibition effect of oxygen at low initiator concentrations. Increasing the initiator concentration also creates an internal filter effect and leads to a reduction in the conversion percentage values.

Finally, the addition of *N*-methyldiethanolamine (MDEA) as co-initiator leads to a drastic increase of the photopolymerization efficiency, as expected for a type II photoinitiator. Comparative experiments were achieved with the thioxanthone parent compound at a concentration value (OD = 0.75) in the presence and absence of MDEA as given in Table 1 (run 6). TX without an amine does not initiate the polymerization of MMA. Conversion of monomer to polymer was very low when TX was used with amine compared to the results obtained with TX-NPG.

Concerning the M_n values, a general trend is noticed as follows: under oxygen, M_n values are low as a consequence of the oxygen inhibition which acts as radical scavenger toward initiating and propagating radicals. When using nitrogen for

dx.doi.org/10.1021/ma302641d | *Macromolecules* XXXX, XXX, XXX−XXX

inerting the sample, this effect disappears and consequently the M_n values increase.

In the presence of MDEA, the efficiency of the initiation process increases due to the formation of aminoalkyl radical. However, in the same time a ketyl radical is formed which is known to act as a terminating agent. Therefore, the M_n values are still relatively low.

Panchromatic photopolymerization experiments were performed in films using different irradiation wavelengths at 392, 473, 532, and 635 nm with an irradiance of 40 mW/cm^2. The ability of TX-NPG to act as radical photoinitiator is exemplified by the conversion curves in Figure 6 and Table 2 which collects

Table 2. Photopolymerization Experiments in Films under Different Irradiation Wavelengths λ_{irr}; [TX-NPG] = 1×10^{-3} M

λ_{irr} (nm)	NPG (mol L^{-1})	conv (%)	$R_p/[M]_0 \times 100$ (s^{-1})
392		63	6.32
	5×10^{-3}	71	12.88
473		21	0.47
	5×10^{-3}	47	4.72
532		24	0.44
	5×10^{-3}	34	2.88
635		14	0.44
	5×10^{-3}	38	5.33

the values of rates of conversion and final conversions at the different wavelengths. Rates of conversion were determined as the maximum slope of the conversion curves obtained by RT-FTIR (Figure 6).

Although relatively low, the conversion of the monomer proves the ability of TX-NPG to form radicals under excitation from UV to red, confirming the above-mentioned mechanism. As can be expected, the reactivity both in terms of conversion and rate of polymerization is quite high at 392 nm, as a consequence of the highest absorption coefficient compared to other wavelengths.

The efficiency of the photopolymerization reaction was found to be drastically enhanced by addition of NPG as a co-initiator (5×10^{-3} M). This beneficial effect can be seen in Figure 6 and Table 2 which shows a significant enhancement of the final conversion for all wavelengths. The rate of conversion also increases by a 2 fold factor at 392 nm and almost a 10-fold factor at 473 nm, 532 and 635 nm. As the triplet state is characterized by a relatively high energy, it is expected that the reactivity under 532 and 635 nm mostly arises from the first excited singlet state S_1. It has been indeed recently shown that singlet excited states of dyes can efficiently initiaite a photopolymerization process.[38]

CONCLUSION

In this article, a new thioxanthone derivative was synthesized which exhibits exceptional absorption properties covering the whole UV−vis spectrum. The energy diagram for the singlet state was clarified, and the involvement of a relatively long-lived triplet state was evidenced. From this triplet state, a photoreduction can occur with an amine, leading to highly efficient initiating radicals. The photopolymerization ability of this new compound was evidenced though gel permeation experiments. Additionally, photopolymerization at different wavelengths covering the electromagnetic spectrum was performed, demonstrating the ability of this compounds to act as a panchromatic photoinitiator.

ASSOCIATED CONTENT

Supporting Information

UV−vis spectrum of TX-NPG in the presence of triethylamine; femtosecond transient spectra and data treatment. This material is available free of charge via the Internet at http://pubs.acs.org.

AUTHOR INFORMATION

Corresponding Author

*E-mail: narsu@yildiz.edu.tr (N.A.); xavier.allonas@uha.fr (X.A.).

Notes

The authors declare no competing financial interest.

ACKNOWLEDGMENTS

N.A. and M.A. thank the Yildiz Technical University Research Fund and TUBITAK for financial support. D.S.E. thanks TUBITAK-BIDEB for financial support.

REFERENCES

(1) Mishra, M. K.; Yagci, Y. In *Handbook of Radical Vinyl Polymerization*; Marcel Dekker Inc.: New York, 1999; Chapter 7.
(2) Green, W. A. In *Industrial Photoinitiators*; CRC Press: Boca Raton, FL, 2010.
(3) Drobny, J. G. In *Radiation Curing for Polymers*, 2nd ed.; CRC Press: Boca Raton, FL, 2010.
(4) Yagci, Y.; Jockusch, S.; Turro, N. J. *Macromolecules* **2010**, *43* (15), 6245−6260.
(5) (a) Dietliker, K. In *A Compilation of Photoinitiators Commercially Available for UV Today*; Sita Technology Ltd.: London, 2001. (b) Fouassier, J. P.; Allonas, X.; Lalevée, J.; Dietlin, C. In *Photochemistry and Photophysics of Polymer Materials*; Wiley: Hoboken, NJ, 2010; pp 351−419.
(6) Decker, C. *Prog. Polym. Sci.* **1996**, *21*, 593.
(7) Davidson, R. S. In *Advances in Physical Chemistry*; Bethel, D., Gold, V., Eds.; Academic Press: London, 1983.
(8) Amirzadeh, G.; Schnabel, W. *Makromol. Chem.* **1981**, *182*, 2821.
(9) Davidson, R. S. In *Radiation Curing in Polymer Science and Technology*; Fouassier, J. P., Rabek, J. F., Eds.; Elsevier Applied Science: London, 1993; Vol. 3, p 153.
(10) Jakubiak, J.; Allonas, X.; Fouassier, J. P.; Sionkowska, A.; Andrzejewska, E.; Linden, L. A.; Rabek, J. F. *Polymer* **2003**, *44* (18), 5219.
(11) Tasdelen, M. A.; Moszner, N.; Yagci, Y. *Polym. Bull.* **2009**, *69*, 173.
(12) O'Brien, A. K.; Cramer, N. B.; Bowman, C. N. *J. Polym. Sci., Part A: Polym. Chem.* **2006**, *44*, 2007.
(13) Courtecuisse, F.; Cerezo, J.; Croutxé-Barghorn, C.; Dietlin, C.; Allonas, X. *J. Polym. Sci., Part A: Polym. Chem.* **2013**, *51* (3), 635−643.
(14) Anderson, D. G.; Davidson, R. S.; Elvery, J. J. *Polymer* **1996**, *37*, 2477.
(15) Timpe, H. J.; Kronfeld, K. P. *J. Photochem. Photobiol., A* **1989**, *46* (2), 253.
(16) Neumann, M. G.; Gehlen, M. H.; Encinas, M. V.; Allen, N. S.; Corrales, T.; Peinado, C.; Catalina, F. *J. Chem. Soc., Faraday Trans.* **1997**, *93*, 1517.
(17) Temel, G.; Arsu, N.; Yagci, Y. *Polym. Bull.* **2006**, *57* (1), 51.
(18) Monroe, B. C.; Weed, G. C. *Chem. Rev* **1993**, *93*, 435.
(19) Fouassier, J. P.; Allonas, X.; Burget, D. *Prog. Org. Coat.* **2003**, *47*, 16.
(20) Mallavia, R.; Fimia, A.; Garcia, C.; Sastre, R. *J. Mod. Opt.* **2001**, *48*, 941.
(21) Zhang, H.; Sheng, Y.; Zhang, G. *J. Optoelectronics, Laser* **2004**, *2*, 29.

(22) Cokbaglan, L.; Yagci, Y.; Jockusch, S.; Turro, N. *Macromolecules* **2003**, *36*, 2649.
(23) Karasu, F.; Arsu, N.; Yagci, Y. *J. App. Polym. Sci.* **2007**, *103*, 3766.
(24) Aydin, M.; Arsu, N.; Yagci, Y. *Macromol. Rapid Commun.* **2003**, *24*, 718.
(25) Karasu, F.; Arsu, N.; Jockusch, S.; Turro, N. *Macromolecules* **2009**, *42*, 7318.
(26) Yilmaz, G.; Aydogan, B.; Temel, G.; Arsu, N.; Moszner, N.; Yagci, Y. *Macromolecules* **2010**, *43*, 4520.
(27) Catalina, F.; Tercero, J. M.; Peinado, C.; Sastre, R.; Mateo, J. L.; Allen, N. S. *J. Photochem. Photobiol., A* **1989**, *50*, 249.
(28) Yilmaz, G.; Acik, G.; Yagci, Y. *Macromolecules* **2012**, *45* (5), 2219.
(29) Rubio-Pons, Ã. S.; Serrano-Andrés, L.; Burget, D.; Jacques, P. *J. Photochem. Photobiol., A* **2006**, *179* (3), 298−304.
(30) Angulo, G.; Grilj, J.; Vauthey, E.; Serrano-Andrés, L.; Rubio-Pons, O.; Jacques, P. *ChemPhysChem* **2010**, *11* (2), 480.
(31) Ley, C.; Morlet-Savary, F.; Jacques, P.; Fouassier, J. P. *Chem. Phys.* **2000**, *255* (2−3), 335.
(32) Ernsting, N. P.; Kovalenko, S. A.; Senyushkina, T.; Saam, J.; Fartzdinov, V. *J. Phys. Chem. A* **2001**, *105*, 3443.
(33) van Stokkum, I. H. M.; Larsen, D. S.; van Grondelle, R. *Biochim. Biophys. Acta* **2004**, *1657*, 824.
(34) Brazard, J.; Ley, C.; Lacombat, F.; Plaza, P.; Martin, M. M.; Checcucci, G.; Lenci, F. *J. Phys. Chem. B* **2008**, *112*, 15182.
(35) Allonas, X.; Ley, C.; Bibaut, C.; Jacques, P.; Fouassier, J. P. *Chem. Phys. Lett.* **2000**, *322*, 483.
(36) Ferreira, G. C.; Schmitt, C. C.; Neumann, M. G. *J. Braz. Chem. Soc.* **2006**, *17* (5), 905.
(37) Allen, N. S.; Mallon, D.; Sideridou, I.; Green, A.; Timms, A.; Catalina, F. *Eur. Polym. J.* **1992**, *28*, 647.
(38) Tarzi, O. I.; Allonas, X.; Ley, C.; Fouassier, J. P. *J. Polym. Sci., Part A: Polym. Chem.* **2010**, *48* (12), 2594−2603.